

See discussions, stats, and author profiles for this publication at: <https://www.researchgate.net/publication/279226455>

Photoresponsive Nanoporous Smectic Liquid Crystalline Polymer Networks: Changing the Number of Binding Sites and Pore Dimensions in Polymer Adsorbents by Light

ARTICLE *in* MACROMOLECULES · JUNE 2015

Impact Factor: 5.8 · DOI: 10.1021/acs.macromol.5b00623

CITATION

1

READS

51

7 AUTHORS, INCLUDING:



[Huub van Kuringen](#)

Technische Universiteit Eindhoven

8 PUBLICATIONS 94 CITATIONS

[SEE PROFILE](#)



[G. Portale](#)

European Synchrotron Radiation Facility

107 PUBLICATIONS 1,190 CITATIONS

[SEE PROFILE](#)



[Dirk Broer](#)

Technische Universiteit Eindhoven

269 PUBLICATIONS 5,084 CITATIONS

[SEE PROFILE](#)



[Albertus P H J Schenning](#)

Technische Universiteit Eindhoven

295 PUBLICATIONS 14,385 CITATIONS

[SEE PROFILE](#)

Photoresponsive Nanoporous Smectic Liquid Crystalline Polymer Networks: Changing the Number of Binding Sites and Pore Dimensions in Polymer Adsorbents by Light

Huub P. C. van Kuringen,^{†,‡} Zino J. W. A. Leijten,[†] Anne Hélène Gelebart,^{†,§} Dirk J. Mulder,^{†,‡} Giuseppe Portale,^{||} Dirk J. Broer,^{*,†,§} and Albertus P. H. J. Schenning^{*,†,§}

[†]Department of Functional Organic Materials and Devices, Chemical Engineering and Chemistry, Eindhoven University of Technology, Den Dolech 2, 5612 AZ, Eindhoven, The Netherlands

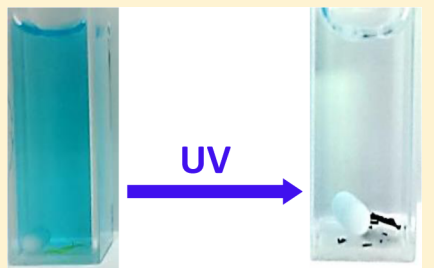
[‡]Dutch Polymer Institute (DPI), PO Box 902, 5600 AX, Eindhoven, The Netherlands

^{*}Institute for Complex Molecular Systems, Eindhoven University of Technology, P.O. Box 513, 5600 MB, Eindhoven, The Netherlands

^{||}DUBBLE-CRG, Netherlands Organization for Scientific Research (NWO), European Synchrotron Radiation Facility (ESRF), Grenoble F-38043, France

S Supporting Information

ABSTRACT: Photoresponsive nanoporous polymer films have been fabricated by adding a photoresponsive azobenzene cross-linker to a hydrogen-bonded smectic liquid crystalline polymer network. A base treatment resulted in the nanoporous material which has been fully characterized. Upon exposure to UV light a decrease in the smectic layer spacing is observed, suggesting a decrease in pore size. In addition, the binding sites in the material could be changed with light, leading to light-induced adsorption of cations and cationic dyes. Finally, light could also be used to create nanoporous channels in the polymer film.



INTRODUCTION

Nanoporous materials have gained considerable attention in the past decade as appealing candidates for adsorption, delivery, and separation of ions and molecules.¹ Such functional materials exhibit high porosity, low density, high specific surface area, and permeability.² In the literature various (porous) materials have been described that show selective adsorption, including silica,³ hydrogels,⁴ metal–organic frameworks, zeolites, and polymers.⁵ Polymers offer advantages over these materials thanks to their versatility in chemistry and processability.

Nanoporous materials based on liquid crystal (LC) polymers are especially appealing thanks to their uniform nanometer pore size, high surface area, and permeability, which promote the adsorption capacity and kinetics.⁶ Nanoporous LC networks have been reported as nanoporous membranes⁷ and (chiral) adsorbents.⁸

A next challenge in this field is to control capture, transport, and release of species in nanoporous materials by an external stimulus.⁹ Various stimuli can be used including pH, light, temperature, magnetic, and electric fields. Among them light is particularly attractive, allowing accurate and remote tuning with high spatial and temporal accuracy.¹⁰ One of the well-known photoresponsive moieties is azobenzene.¹¹ This photochromic dye can undergo a trans–cis isomerization upon light irradiation causing a change in size, conformation, and dipole

moment.^{11,12} Isomerization of azobenzene compounds can lead to photochromic pK_a changes,¹³ which might lead to a change in adsorption binding strength. When incorporated in a host molecule, the pore dimension can be changed driving its selectivity toward cations with different size.^{14,15}

Azobenzene molecules have been applied in liquid crystals and liquid crystal polymers¹⁶ to combine photoresponse with self-organization of molecules.^{11a} However, photoresponsive nanoporous LC materials have only been rarely reported. Gas permeation LC membranes have been prepared which can switch between an impermeable ordered state and a permeable disordered state¹⁷ while azobenzene containing smectic LCs have been used to induce anisotropic ion conduction and photoswitchable ion conduction.¹⁸ Lyotropic azobenzene containing LC assemblies with switchable nanopores have also been reported.¹⁹

Previously, we have reported on nanoporous smectic LC polymer network based on the self-organization of reactive thermotropic hydrogen-bonded smectic liquid crystals as a very efficient adsorbent.⁶ The anionic pore interior of this nanoporous material was able to selectively adsorb cationic dyes such as methylene blue which could be retrieved after acid

Received: March 25, 2015

Revised: May 13, 2015

Published: June 9, 2015

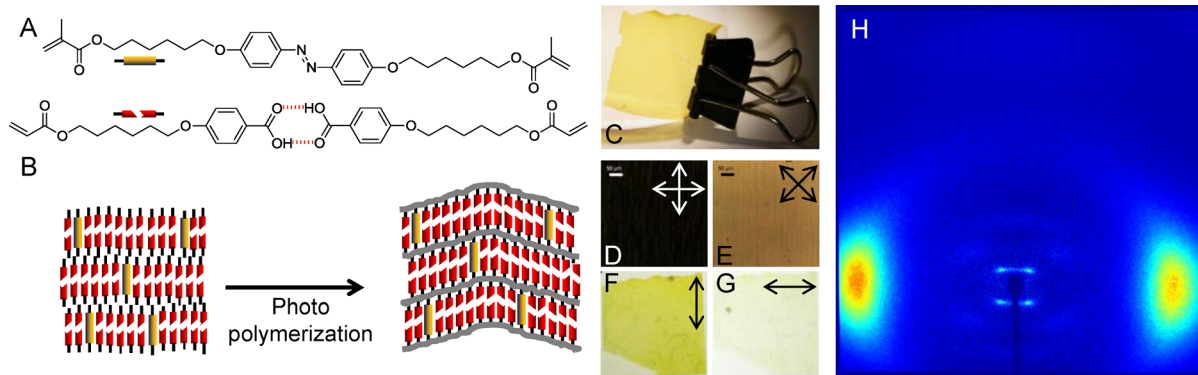


Figure 1. (A) Chemical structure of A6MA and 6OBA dimer. (B) Schematic representation of the formation of the polymer network causing a change in molecular organization. (C) The free-standing hydrogen-bonded polymer film. (D, E) POM images taken between crossed polarizers. The aligned azobenzene cross-linker in the polymerized film exhibits dichroism under 0° (F) and 90° (G) polarizers. (H) XRD picture of the polymer film showing the smectic C structure. The molecular director in (D, E, F, G, and H) is in the same direction as depicted in (B).

treatment of the polymer. We now report on photoresponsive nanoporous LC materials by incorporating a photoresponsive azobenzene cross-linker to the hydrogen-bonded smectic liquid crystalline polymer network. In order to create nanopores, the polymer network is treated with a base leading to the breakup of the hydrogen bonds and a photoresponsive smectic nanoporous material. Interestingly, upon light exposure the lamellar spacing decreases as a result of the trans–cis isomerization. Remarkably, the number of binding sites in this material can also be controlled, resulting in light controlled adsorption of cations and cationic dyes. Finally, light is used to fabricate nanoporous channels in the polymer film.

EXPERIMENTAL SECTION

Materials. The photoresponsive cross-linker, 4,4'-bis(6-methacryloxyhexyloxy)azobenzene (A6MA), was synthesized by Philips Research Laboratories.²⁰ The hydrogen-bonded 4-(6-acryloyloxyhexyloxy)benzoic acid (6OBA) was custom-made by Synthon Chemicals, Germany. The initiator, bis(2,4,6-trimethylbenzoyl)-phenylphosphine oxide (Irgacure 819), was supplied by Ciba Specialty Chemicals, and the inhibitor *p*-methoxyphenol was purchased from Sigma-Aldrich.

Preparation of the Liquid Crystalline Monomer Mixture. A LC mixture was made from the hydrogen-bonded 6OBA and the covalently bonded photoresponsive cross-linker A6MA, in a 95/5 molar ratio. In order to make the mixture accessible for photo-polymerization, 0.5 wt % photoinitiator was added and 0.1 wt % of *p*-methoxyphenol was added as thermal polymerization inhibitor. The mixture was made by dissolving the compounds in dichloromethane, which was subsequently evaporated.

Photopolymerization. Films with a thickness of 6 or 18 μm were obtained by capillary suction of the mixture in the melt at 100 °C between two accurately spaced glass plates. The glass plates were provided with rubbed polyimide (OPTIMER AL 1051, JSR Corporation, Tokyo, Japan) to obtain planar alignment. The glass cell was cooled to 90 °C at 5 °C/min followed by an isotherm of 2 min. The photopolymerization in the smectic state of the monomers was performed for 1000 s with a mercury lamp (Omnicure s1000, emitting at 320–500 nm) which was provided with a 400 nm cutoff filter (Newport), to avoid the isomerization of the azobenzene moiety during polymerization. The intensity was approximately 22 mW cm^{-2} at the sample surface. To ensure maximum conversion of the acrylate bonds, the polymerization was followed by a heat treatment at 135 °C for 15 min.

Deprotonation and Protonation. The polymer network was cut in small pieces to obtain polymer flakes which were (5 × 5 mm, 0.5/1.0 mg) immersed in 5 mL buffered sodium borate solutions ($\text{pH} = 7$

until 10) or 0.1 M KOH ($\text{pH} = 13.0$) to deprotonate the benzoic acid moieties, leading to the breaking of the hydrogen bonds. The protonation process was done in 5 mL buffered solutions or 0.1 M HCl ($\text{pH} = 1.0$). The films were kept 1 day in the KOH and HCl solutions and 3 days in the buffered solutions to equilibrate the system.

Isomerization. The isomerization of the azobenzene LC network was investigated using the mercury lamp provided with a UV band-pass filter (<400 nm). The emitted intensity was approximately 25 mW cm^{-2} . Polymer flakes were immersed in the buffered solution, irradiated, and stirred continuously.

Adsorption. The adsorption process was performed with the cationic dye, methylene blue (MB) (Acros Organics). Polymer films were exposed to a freshly made, 5 $\mu\text{g}/\text{mL}$ MB buffered sodium borate solution.

Characterization. Fourier transform infrared spectroscopy (FTIR) spectra were obtained using a FTS 6000 spectrometer from Bio-Rad equipped with Specac Golden gate diamond ATR and were signal-averaged over 50 scans at a resolution of 1 cm^{-1} . Varian Resolution Pro software was used for the analysis of the spectra. Polarized optical microscopy (POM) studies were conducted using a Leica CTR 6000 microscope equipped with two polarizers that were operated either crossed or parallel with the sample in between a Linkam hot-stage THMS600 with a Linkam TMS94 controller and a Leica DFC420 C camera. A DSC-Q1000 from TA Instruments was used with 1 °C/min temperature ramp ranging from 0 °C until 140 °C and 3 min isotherm. The second cycle was used for characterization. POM samples were prepared between a not rubbed polyimide coated glass plate and a not coated cover glass. X-ray diffraction (XRD) of the monomer mixture was performed on a Ganesha lab instrument equipped with a Genix-Cu ultralow divergence source producing X-ray photons with a wavelength of 1.54 Å and a flux of 1×10^8 photons/s. Scattering patterns were collected using a Pilatus 300 K silicon pixel detector with 487 × 619 pixels of 172 μm^2 in size. A glass capillary was filled with the monomer mixture and heated with 30 °C/min until the isotropic phase was reached and subsequently cooled with 10 °C/min. Pictures were recorded for 5 min. XRD experiments on polymer films at middle and wide angles have been performed at the DUBBLE-BM26B beamline at the ESRF, Grenoble, France.²¹ An X-ray wavelength λ of 1.033 Å and a sample-to-detector distance of about 20 cm were used. 2D images have been recorded using a Frelon CCD detector with pixel size of 43.88 × 43.88 μm and dimension 2048 × 2048 pixels. The CCD detector has been used in binning 2 × 2 mode. Images have been corrected for the incoming beam intensity, background scattering, and sample absorption. After all the corrections have been applied, 2D images have been integrated along the same angular sector in order to obtain the $I(q)$ vs q 1D profiles. The q scale (where q is the module of the scattering vector and is equal to $4\pi/\lambda \sin(\theta)$, with θ being half of the scattering angle). Polymer films were placed in the beam using a small holder equipped with two thin mica windows.

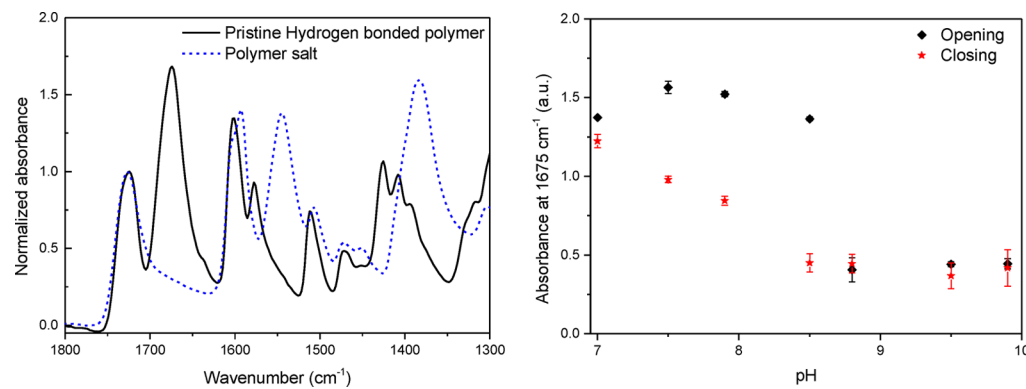


Figure 2. Left: FTIR spectra of the pristine hydrogen-bonded polymer network and the polymer salt network. Right: FTIR absorbance at 1675 cm^{-1} of the polymer film of the cycle of deprotonation (opening) by increasing pH and protonation (closing) by decreasing pH.

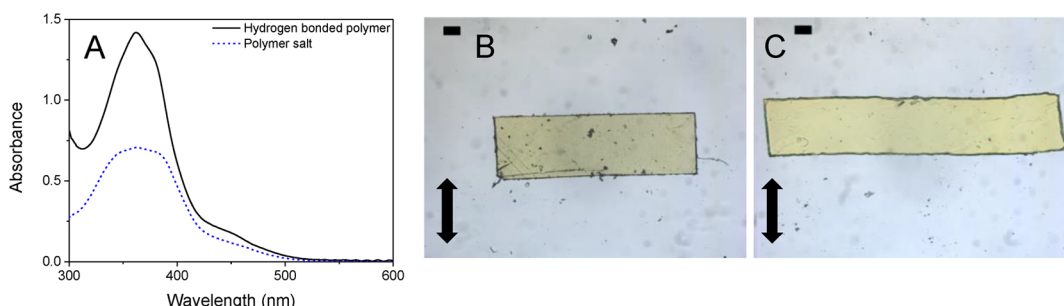


Figure 3. UV-vis spectra (A) and microscope pictures of the hydrogen-bonded polymer film (B) and swollen polymer salt film (C). The alignment direction is indicated by the arrows; the scale bar is $100\text{ }\mu\text{m}$.

The exposure time was 60 s per image. All spectra were smoothed to remove spikes. Absorbance measurements of the polymer films and dye absorption measurements of solutions were performed in 1 cm path length quartz cells and using an UV-vis-NIR spectrophotometer (Shimadzu UV-3102).

RESULTS AND DISCUSSION

Fabrication of Nanoporous LCs Polymer Network. For making the photoresponsive nanoporous network a LC mixture (Figure 1A) was used containing a photoresponsive azobenzene diacrylate cross-linker (A6MA, molecular length in extended conformation is 3.6 nm) and a hydrogen-bonded dimer diacrylate (6OBA dimer, molecular length in extended conformation is 3.9 nm) in a 5/95 molar ratio. The phase behavior of this mixture was characterized with DSC, POM, and XRD. DSC revealed upon heating a melting peak at $89\text{ }^{\circ}\text{C}$ followed with two mesophase transitions (Figure S1). Upon cooling the mixture exhibited a smectic A phase at $97\text{ }^{\circ}\text{C}$, and it crystallized at $58\text{ }^{\circ}\text{C}$ (Figure S1). The phase transitions are similar to 6OBA mixed with a nonphotoresponsive cross-linker having a similar length and shape.⁶ The smectic phase was confirmed with XRD. An intermolecular spacing of 0.4 nm and a *d*-spacing (layer spacing) of 4.1 nm were calculated (Figure S2). The latter is in close agreement with the estimated molecular length of the 6OBA dimer, which embody 90% of the LCs in the mixture, indicating a lamellar SmA arrangement. The mixture was incorporated in a liquid crystal cell having planar alignment layers and was photopolymerized in the smectic phase at $90\text{ }^{\circ}\text{C}$. After opening of the cell, a planar aligned free-standing polymer film of approximately $2.5 \times 2.5\text{ cm}$ in size was obtained (Figure 1C). FTIR confirmed the conversion of the C=C bond of the acrylate groups at 1635 cm^{-1} (Figure S3) and the presence of the hydrogen bonds (*vide infra*).

The polymer film revealed a homogeneous yellow color, indicating that the azobenzene dye is equally distributed throughout the film. UV-vis spectroscopy measurements (Figure 3A) showed a typical azobenzene absorbance spectra,^{12b} with an intense $\pi \rightarrow \pi^*$ band at 361 nm, corresponding to the trans isomer and a much weaker $n \rightarrow \pi^*$ band at longer wavelengths. POM pictures taken between crossed polarizers showed birefringence, indicating that the material is aligned (Figure 1D,E). Observations with polarized light from a single polarizer showed that the azobenzene cross-linker is coaligned (Figure 1F,G), since the photochromic dye only absorbs light parallel to the molecular axis. XRD measurements showed four lobes featured at middle angles, suggesting a planar aligned polymer film with a typical smectic C organization (Figure 1H). This means upon polymerization that the polymer layers are diagonally oriented in chevron-like fashion (Figure 1B).^{6,22} A narrow signal was found for the intermolecular distance (0.4 nm), and a *d*-spacing of 3.2 nm with a tilt of 41° with respect to the initial SmA organization was observed. The tilted *d*-spacing corresponds well with the molecular length of the 6OBA dimer.

The pH at which the hydrogen bonds are broken was determined by immersing the material in buffered solutions and followed with FTIR (Figure 2). For pristine hydrogen-bonded polymer films the signals at 1675 and 1425 cm^{-1} , corresponding to the carbonyl bond in the hydrogen-bonded state and in-plane bending of the O-H bond, respectively, disappeared at $\text{pH} = 9$. Simultaneously, two new vibrations emerged at $\nu_s = 1540\text{ cm}^{-1}$ and $\nu_{as} = 1385\text{ cm}^{-1}$ and started to appear at $\text{pH} = 9$ to reach a maximum intensity at $\text{pH} = 9.5$. This indicates the formation of a carboxylate salt.²³ Since the asymmetric carboxylic acid vibration at 1675 cm^{-1} is completely vanished after the deposition in basic solution, it can be

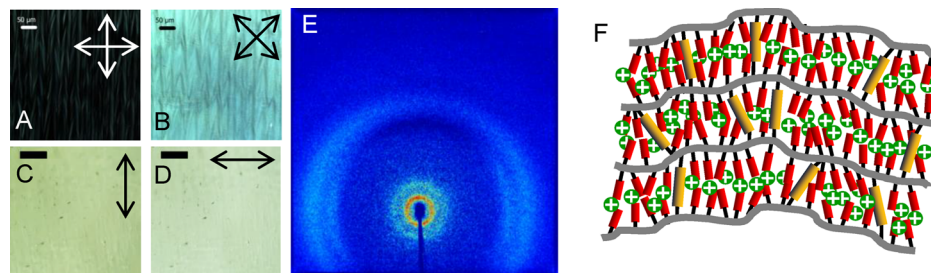


Figure 4. POM pictures of the polymer salt network taken between crossed polarizers (A, B, arrows indicate polarization direction). The scale bar is 50 μm . The aligned azobenzene cross-linker in the polymerized film exhibits marginal dichroism under (C) 0° and (D) 90° polarizers. (E) XRD picture of the polymer salt network. (F) Proposed model of the polymer salt network.

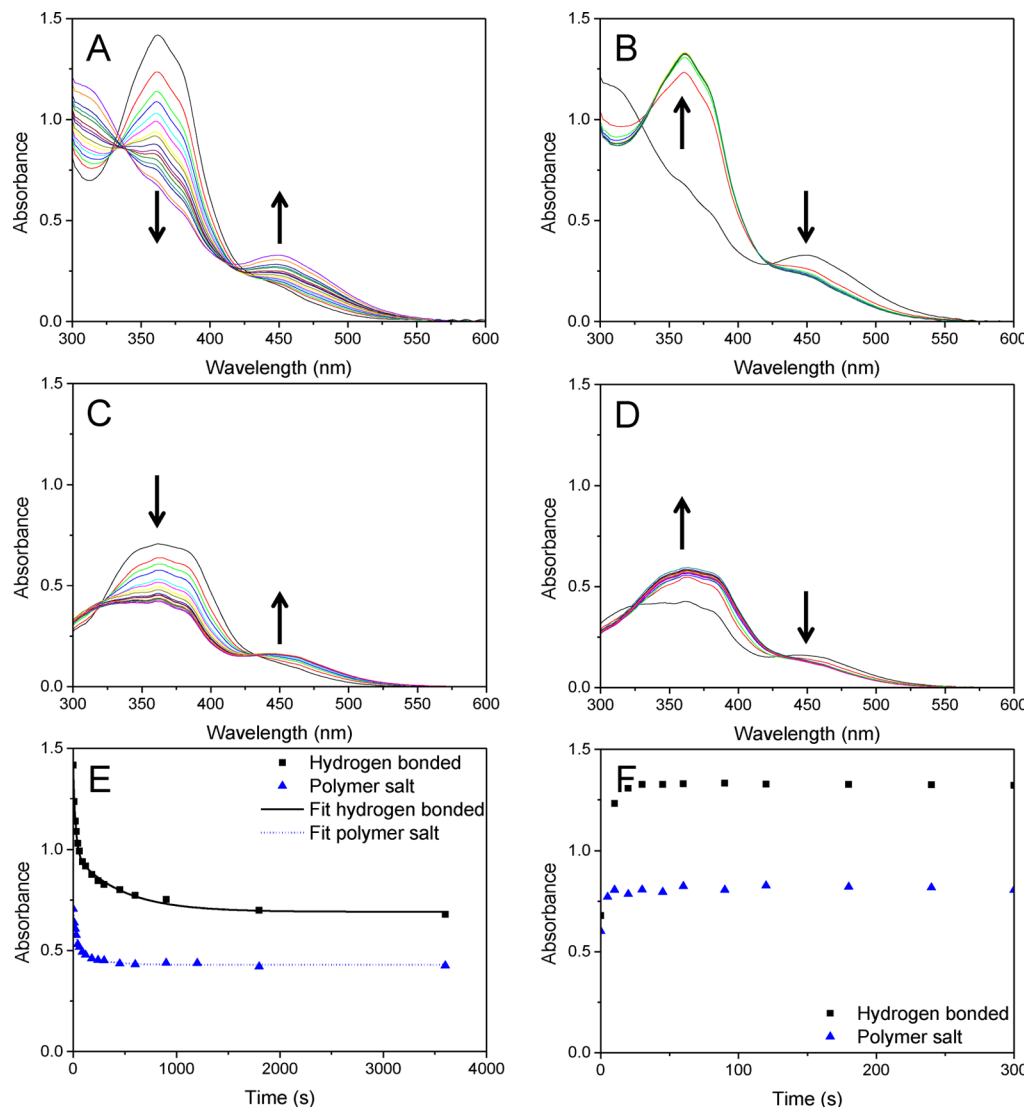


Figure 5. Isomerization of azobenzene induced with light at room temperature measured with UV-vis spectroscopy. (A) and (B) hydrogen-bonded polymer network and (C) and (D) polymer salt network. (E) and (F) the absorbance at 361 nm over time. The plots on the left represent the trans-cis isomerization. The plots on the right are from the cis-trans isomerization.

assumed that the conversion to the polymer salt is completed. In a second step the films—which were completely converted to the polymer salt—were immersed in lower pH solution. While decreasing the pH the vibrations at 1540 and 1385 cm^{-1} started to disappear at pH 8.5 and are completely absent at pH 7 and lower. However, the vibration at 1675 cm^{-1} already appeared at pH 8 and lower. This indicates that the hydrogen

bonds can be formed again and that this process occurs in two steps: (1) protonation of the carboxylate moieties followed with (2) the formation of hydrogen bonds. The latter signal does not reach its original height. This could be attributed to a decreased ordering of the tethers causing changes in the deprotonation process. This is why a second and third cycle of high and low pH treatment were performed. The trend was the

same for both the breaking and the formation of the hydrogen bonds over both cycles, despite the fact that the deprotonation occurs at slightly lower pH (8.5 instead of 9) for the second and third cycle compared to the first one. This demonstrated the reversibility of the pH response after the first cycle. A hysteresis was found between the pH of formation and rupture of the hydrogen bonds (Figure 2).

The polymer salt film showed a severe anisotropic swelling (Figure 3B,C) similar to earlier reported smectic 6OBA polymer films lacking the azobenzene cross-linker.²⁴ The swelling mainly occurred perpendicular to the alignment direction of the LCs, and microscopy pictures revealed a macroscopic size increase of 43% ($\pm 10\%$). Parallel to the alignment direction a 7% ($\pm 6\%$) decrease was observed. UV-vis absorbance of the polymer salt film is less intense (Figure 3A). This is caused by swelling of the polymer film and a loss of order of the azobenzene moiety (*vide infra*).

XRD revealed an almost isotropic signal for both the intermolecular and the layer distance (Figure 4E, Figures S4 and S5), and small deviations of the intensity are found over the rings. The *d*-spacing is 3.5 nm, which is close to the estimated length of the azobenzene cross-linker in the trans state. Observations with polarized light revealed that there is little dichroism remaining (Figure 4C,D), indicating that the azobenzene cross-linker is practically macroscopically unaligned since the photochromic dye only absorbs light which is parallel to the molecular axis. This confirmed the observations from XRD. However, POM pictures taken between crossed polarizers (Figure 4A,B) clearly show the birefringence, indicating that some alignment of the cross-linker is still left. These observations could be explained with a multidomain smectic A undulating layer model²⁵ drawn in Figure 4F. Macroscopically the material is hardly aligned, but within the domains some anisotropy is left, resulting in birefringence. The dimensions ($1.53 \times 10^{-5} \text{ cm}^3$) and layer spacing characteristics of the swollen polymer salt network point to a 2D pore surface area of 8.75 cm^2 .

Photoresponsive Behavior. The photoresponsive properties of the free-standing polymer network films were investigated by a variety of techniques. UV light in the wavelength range of 320–400 nm was used to perform trans–cis isomerization of the azobenzene cross-linker. UV-vis spectroscopy measurements revealed a large decrease of the trans peak at 361 nm and the appearance of the cis isomer peak at 446 nm for both the hydrogen bonded and the polymer salt networks (Figure 5A,C). These are typical observations for the isomerization of azobenzene^{12b} and proof that the isomerization occurs. However, exact values for the conversion cannot be given due to the difficulties in determining the initial trans–cis ratio and the extinction coefficients, caused by changes in volume and orientation of the azobenzene in the anisotropic films. The kinetics of the photoresponsive was analyzed by plotting the absorbance at 361 nm as a function of time (Figure 5E). This revealed a steep slope in the first seconds followed by a flattening, indicating that a photostationary state is reached.

The isomerization kinetics can be described by the following equation which has been used to study the isomerization of azobenzene in thin (glassy) polymer films.^{26,27}

$$\frac{A_\infty - A_t}{A_\infty - A_0} = \alpha \exp(k_f t) + (1 - \alpha) \exp(k_s t) \quad (1)$$

A_0 , A_t , and A_∞ represent the absorbance at the initial state, at time t (s), and at infinite time, respectively. k_f and k_s embody a fast and slow rate constant (s^{-1}), and α is the fraction that underwent the fast reaction. This model divides the isomerization kinetics into two first-order reactions. The rate constants were determined and are summarized in Table 1.

Table 1. Kinetic Parameters of the Light-Induced Isomerization in the Hydrogen-Bonded and Polymer Salt Film Using Eq 1

	A_∞	α	$k_f (\times 10^{-3}) \text{ (s}^{-1}\text{)}$	$1 - \alpha$	$k_s (\times 10^{-3}) \text{ (s}^{-1}\text{)}$
H-bonded polymer	0.69	0.6	-42.1	0.4	-2.2
polymer salt	0.42	0.7	-33.1	0.3	-5.0

The calculation can be found in the Supporting Information. These typical values²⁶ reveal that the rate constants are on the same order of magnitude and that two processes play a significant role. For the hydrogen-bonded network k_f is higher, while k_s is higher for the polymer salt network. The underlying mechanism could be based on mobility arguments, which are higher in the state where the hydrogen bonds are broken. But in addition, this swollen polymer salt system is known to stretch the bridging cross-linker to a smectic A configuration, as confirmed by the XRD data.²² In our system the azobenzene compound is the cross-linker which is stretched along the long axis, thus bringing the azo moiety under stress, especially in the cis state, leading to an anticipated mechanical–chemical acceleration of the back-reaction. This could also explain the smaller decrease of the trans signal in the polymer salt state at photostationary conditions.

The back-isomerization can occur by thermal relaxation and exposure to visible light. Blue light irradiation at room temperature revealed a very fast response (Figure 5B,D,F). Within 20 s both networks reached a photostationary state. Remarkably, the absorbance does not reach the same value as the pristine films. The films were also allowed to relax back at room temperature in the dark (Figure S6). This revealed a slow process which took tens of hours. This allows us to investigate the UV-exposed films with other techniques without large changes in the trans–cis ratio in the material.

Pore Size Changes. XRD measurements (Figure 6) on the polymer salt network revealed that after UV irradiation the *d*-spacing is 3.3 nm, which is 0.2 nm smaller than before. This might be caused by the molecular length change of the azobenzene cross-linker under UV exposure. However, the isomerization of the azobenzene moiety itself is known to cause a molecular length change of 0.35 nm.^{12b} This discrepancy could be attributed to the fraction of azobenzene units which were not isomerized to the bended cis state, and the flexibility of the main chain between two azobenzene units could allow deformation. This measurement was performed with the same polymer salt film as before (Figure 4E) which was shielded by a mica window during both measurements to prevent water evaporation. Furthermore, the signal at 18.5 nm^{-1} is more pronounced and could be attributed to water. This could mean that water is squeezed out of the nanostructured material. Although the humidity has played a role by inducing some limitations in measuring conditions, it is the first indication that the isomerization of azobenzene changed the *d*-spacing in smectic liquid crystalline polymer networks and could indicate the formation of smaller pores.

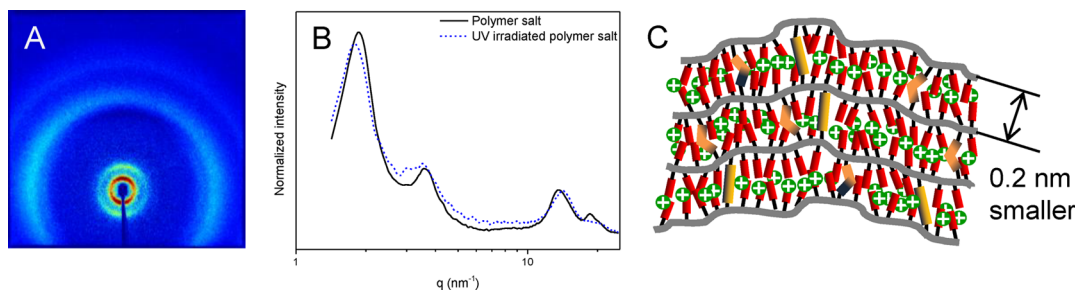


Figure 6. XRD image from the UV-irradiated polymer salt film (A) and the 1D profiles of the UV irradiated and not irradiated polymer salt film (B). The layer spacing is 0.2 nm smaller after UV irradiation (C).

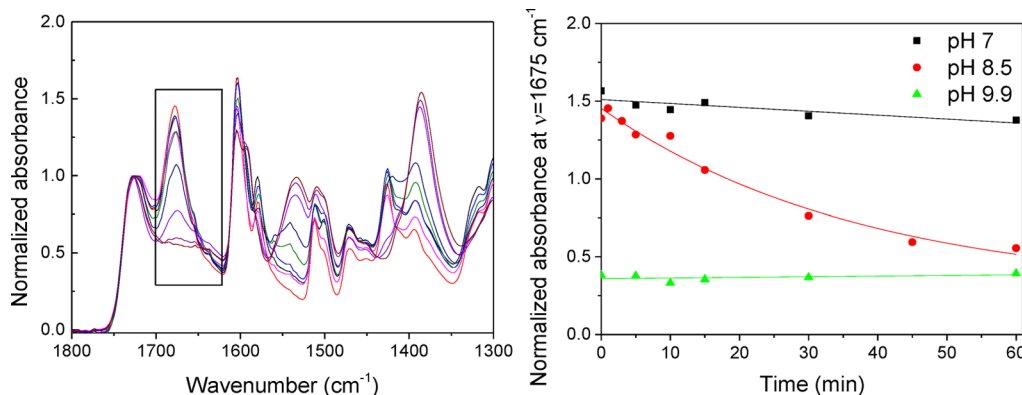


Figure 7. Left: FTIR spectra taken from the irradiated hydrogen-bonded polymer film at pH 8.5 Right: the intensity of the absorbance at 1675 cm^{-1} during isomerization of azobenzene in buffered solutions.

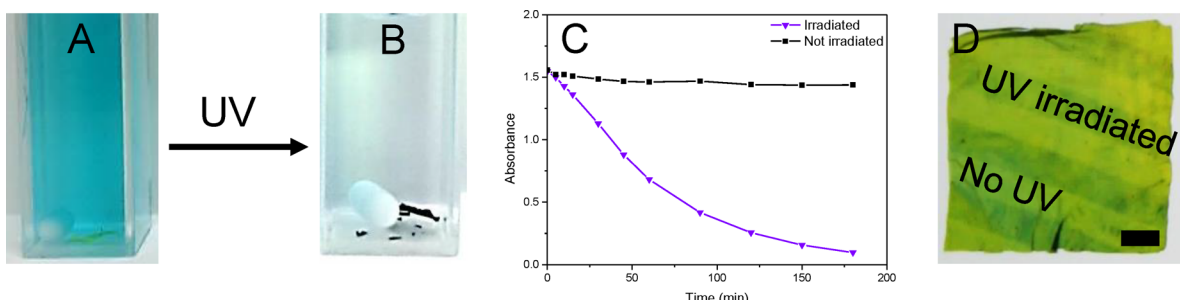


Figure 8. Photoinduced adsorption of MB. The hydrogen-bonded polymer film does not adsorb MB (A). Exposure of this polymer film to UV light results in the adsorption of MB (B). Change of absorbance of MB over time for both the light exposed and nonexposed polymer films (C). Locally irradiated polymer film that only adsorb at the illuminated areas (D). The scale bar is 1 mm.

The 5% decrease in d -spacing did not result in a macroscopic change that could be observed with the naked eye. Optical microscopy pictures also did not show observable dimensional changes upon irradiation (Figures S7 and S8). Because of relatively low concentration of azobenzene, one could expect shrinkage and expansion in the direction parallel and perpendicular to the molecular director, respectively.^{28,29} Adsorption experiments revealed that the adsorption of methylene blue (MB)⁶ was not influenced by light meaning that binding sites are equally accessible for this dye (Figure S9).

Change in Binding Sites. The influence of the isomerization of azobenzene on the number of binding sites was explored by exposing the polymer film to a certain pH and simultaneous light irradiation. Buffer solutions were selected so that the resulting films were in the hydrogen-bonded state, in the polymer salt state, and at the edge between hydrogen-bonded and polymer salt, but still in the hydrogen-bonded regime, at pH 7.0, 9.9, and 8.5, respectively (Figure 2). Polymer

films underwent an alkaline and acid treatment prior to use. This was done to erase the initial molecular ordering and get in the reversible regime. Subsequently, the films were immersed in buffer solution and allowed to equilibrate for a day before they were irradiated with UV light at room temperature. IR spectra were recorded during 60 min of UV irradiation. No changes were found in these spectra for the material at pH 7.0 and 9.9 (Figures S7 and S8). Interestingly, the film in pH 8.5 solution revealed a gradual change in the vibrations at 1675, 1540, 1425, and 1385 cm^{-1} (Figure 7), showing that hydrogen bonds were converted to the polymer salt during UV irradiation. This is slower than the isomerization of azobenzene (Figure 5E) and could be attributed to a slower diffusion of ions. This conversion is most likely caused by the change in dipole moment of the isomerized azobenzene cross-linker, which causes a change of the pK_a of the benzoic acid moieties, resulting in the formation of a nanoporous polymer salt film. Photochromic pK_a changes in azobenzene molecules have been

reported.¹⁵ Remarkably, in our case photochromic changes lead to the formation of binding sites in the polymer material. It should be noted that an elevated temperature, caused by the thermal heating of the sample by illumination, does not affect the process (Figure S10). Light-controlled release of ions was investigated as well. UV-exposed polymer salt films at pH 8.5 were irradiated with blue light to induce the back-isomerization. This resulted in the cis–trans isomerization of the azobenzene, but no hydrogen bonds were re-formed and no ions were released. This is most likely caused by the hysteresis as earlier observed (Figure 2). Lowering of the pH is necessary to release ions.

The photoinduced creation of binding sites can be visualized with the adsorption of MB. Therefore, MB was added to the pH 8.5 buffer and the pretreated hydrogen bonded film was immersed in the blue 3 mL 5 µg/mL MB solution and irradiated with UV light for 3 h while being stirred. The solution became gradually less blue, and the film appeared blue (Figure 8A,B). Absorbance spectra were recorded of the solution *in situ* with UV-vis spectroscopy, confirming the decrease of MB in solution (Figure 8C). A similar experiment was performed with a pretreated hydrogen-bonded polymer film in MB buffer solution, but without the UV irradiation step. This solution is still blue after 3 h, and UV-vis measurements revealed only a small decrease of MB in solution, indicating that this film hardly adsorbs MB. UV irradiation of a MB buffer solution without adsorbent revealed a marginal decrease of the MB absorbance signal (Figure S11), indicating that (photo) reduction of MB barely occurred.³⁰

We have also investigated if light can be used to create a nanoporous pattern in the hydrogen-bonded polymer film. Therefore, a polymer film was covered with a lined photomask, irradiated for 1 h and subsequently immersed in a MB solution. Figure 8D shows that only the areas which have been illuminated have adsorbed MB. This shows that a light stimulus can create nanopores in a polymer films and show the merits of using light as local stimulus to control transport in a polymer material.

CONCLUSIONS

Our work shows photoresponsive nanoporous LC polymer films which can be fabricated by incorporation of an azobenzene cross-linker in a smectic liquid crystalline hydrogen-bonded polymer network and subsequent treatment with an alkaline solution. Interestingly, upon exposure to UV light a decrease of the smectic layer spacing in polymer salt network is observed, suggesting that the pore size alters. Although preliminary show no change of the adsorption toward cationic dyes, such a result is interesting to control capture and release of species. Moreover, the isomerization of azobenzene moieties leads to a change in the number of the binding sites, resulting in light-induced adsorption of cations and cationic dyes. This effect is most likely due to a change in dipole moment of the azobenzene cross-linker, leading to a change of the pK_a of the surrounding benzoic acid moieties. Such a mechanism is novel and should be taken into account in porous materials that show light-induced adsorption, transport, and release of species. The absorbed cations can in principle be released again by lowering the pH, which makes these materials appealing for the recovery of valuable species or for cleaning purposes. Light can also be used to create nanoporous channels in a polymer film, showing that this method can be potentially used to control transport of species in polymer materials.

ASSOCIATED CONTENT

Supporting Information

Additional monomer and material characterization, derivation of the kinetics, and an adsorption study. The Supporting Information is available free of charge on the ACS Publications website at DOI: 10.1021/acs.macromol.5b00623.

AUTHOR INFORMATION

Corresponding Authors

*E-mail d.broer@tue.nl (D.J.B.).

*E-mail a.p.h.j.schenning@tue.nl (A.P.H.J.S.).

Notes

The authors declare no competing financial interest.

ACKNOWLEDGMENTS

This research forms part of the research programme of the Dutch Polymer Institute (DPI), project 742. We thank My Phung Van for performing XRD measurements on the monomer mixture. NWO is acknowledged for making the beam time available at the ESRF.

REFERENCES

- (1) Mohmood, I.; Lopes, C. B.; Lopes, I.; Ahmad, I.; Duarte, A. C.; Pereira, E. *Environ. Sci. Pollut. Res.* **2013**, *20*, 1239–1260.
- (2) (a) Ning, Y.; Yang, Y.; Wang, C.; Ngai, T.; Tong, Z. *Chem. Commun.* **2013**, *49*, 8761–8763. (b) van Kuringen, H. P. C.; Schenning, A. P. H. J. In *Hydrogen Bonded Supramolecular Materials*; Li, Z. T., Wu, L. Z., Eds.; Springer: Heidelberg, 2015; p 44.
- (3) Ho, K. Y.; McKay, G.; Yeung, K. L. *Langmuir* **2003**, *19*, 3019–3024.
- (4) (a) Wang, R.; Yu, B.; Jiang, X.; Yin, J. *Adv. Funct. Mater.* **2012**, *22*, 2606–2616. (b) Li, B.; Jiang, X.; Yin, J. *J. Mater. Chem.* **2012**, *22*, 17976–17983. (c) Deng, S.; Xu, H.; Jiang, X.; Yin, J. *Macromolecules* **2013**, *46*, 2399–2406. (d) Deng, S.; Wang, R.; Xu, H.; Jiang, X.; Yin, J. *J. Mater. Chem.* **2012**, *22*, 10055–10061. (e) Paulino, A. T.; Guilherme, M. R.; Reis, A. V.; Campese, G. M.; Muniz, E. C.; Nozaki, J. *J. Colloid Interface Sci.* **2006**, *301*, 55–62.
- (5) (a) Sun, C.-Y.; Wang, X.-L.; Qin, C.; Jin, J.-L.; Su, Z.-M.; Huang, P.; Shao, K.-Z. *Chem.—Eur. J.* **2013**, *19*, 3639–3645. (b) Pu, F.; Liu, X.; Xu, B. L.; Ren, J. S.; Qu, X. G. *Chem.—Eur. J.* **2012**, *18*, 4322–4328.
- (6) (a) van Kuringen, H. P. C.; Eikelboom, G. M.; Shishmanova, I. K.; Broer, D. J.; Schenning, A. P. H. J. *Adv. Funct. Mater.* **2014**, *24*, 5045–5051. (b) Sorenson, G. P.; Schmitt, A. K.; Mahanthappa, M. K. *Soft Matter* **2014**, *10*, 8229–8235.
- (7) (a) Gin, D. L.; Lu, X.; Nemade, P. R.; Pecinovsky, C. S.; Xu, Y.; Zhou, M. *Adv. Funct. Mater.* **2006**, *16*, 865–878. (b) Schenning, A. P. H. J.; Gonzalez-Lemus, Y. C.; Shishmanova, I. K.; Broer, D. J. *Liq. Cryst.* **2011**, *38*, 1627–1639. (c) Zhang, H.; Li, L.; M?ller, M.; Zhu, X. M.; Rueda, J. J. H.; Rosenthal, M.; Ivanov, D. A. *Adv. Mater.* **2013**, *25*, 3543–3548. (d) Henmi, M.; Nakatsuji, K.; Ichikawa, T.; Tomioka, H.; Sakamoto, T.; Yoshio, M.; Kato, T. *Adv. Mater.* **2012**, *24*, 2238–2241. (d) Feng, X.; Tousley, M. E.; Cowan, M. G.; Wiesnauer, B. R.; Nejati, S.; Choo, Y.; Noble, R. D.; Elimelech, M.; Gin, D. L.; Osuji, C. O. *ACS Nano* **2014**, *8*, 11977–11986.
- (8) Ishida, Y. *Materials* **2011**, *4*, 183–205.
- (9) (a) Zhai, L. *Chem. Soc. Rev.* **2013**, *42*, 7148–7160. (b) Jochum, F. D.; Theato, P. *Chem. Soc. Rev.* **2013**, *42*, 7468–7483.
- (10) Zhang, S.; Peng, Y.; Jiang, W.; Liu, X.; Song, X.; Pan, B.; Yu, H.-Q. *Chem. Commun.* **2014**, *50*, 1086–1088.
- (11) (a) Natanson, A.; Rochon, P. *Chem. Rev.* **2002**, *102*, 4139–4176. (b) El Halabieh, R. H.; Mermut, O.; Barrett, C. J. *Pure Appl. Chem.* **2004**, *76*, 1445–1465.
- (12) (a) Nicoletta, F. P.; Cupelli, D.; Formoso, P.; De Filpo, G.; Colella, V.; Gugliuzza, A. *Membranes* **2012**, *2* (1), 134–97. (b) Merino, E.; Ribagorda, M. *Beilstein J. Org. Chem.* **2012**, *8*, 1071–90.

- (c) Banghart, M.; Borges, K.; Isacoff, E.; Trauner, D.; Kramer, R. H. *Nat. Neurosci.* **2004**, *7*, 1381–1386. (d) Liu, N. G.; Dunphy, D. R.; Atanassov, P.; Bunge, S. D.; Chen, Z.; Lopez, G. P.; Boyle, T. J.; Brinker, C. J. *Nano Lett.* **2004**, *4*, 551–554. (e) Barrett, C. J.; Mamiya, J.-i.; Yager, K. G.; Ikeda, T. *Soft Matter* **2007**, *3*, 1249–1261. (f) Pearn, J.; Sun, L.-B.; Chen, Y.-P.; Perry, Z.; Zhou, H.-C. *Angew. Chem., Int. Ed.* **2014**, *53*, 5842–5846.
- (13) Fukaminato, T.; Tateyama, E.; Tamaoki, N. *Chem. Commun.* **2012**, *48*, 10874–10876.
- (14) Natali, M.; Giordani, S. *Chem. Soc. Rev.* **2012**, *41* (10), 4010–4029.
- (15) Gong, C. B.; Lam, M. H. W.; Yu, H. X. *Adv. Funct. Mater.* **2006**, *16*, 1759–1767.
- (16) Yu, H. *J. Mater. Chem. C* **2014**, *2*, 3047–3054.
- (17) (a) Liu, J.; Wang, M.; Dong, M.; Gao, L.; Tian, J. *Macromol. Rapid Commun.* **2011**, *32*, 1557–1562. (b) Glowacki, E.; Horovitz, K.; Tang, C. W.; Marshall, K. L. *Adv. Funct. Mater.* **2010**, *20*, 2778–2785.
- (18) (a) Soberats, B.; Uchida, E.; Yoshio, M.; Kagimoto, J.; Ohno, H.; Kato, T. *J. Am. Chem. Soc.* **2014**, *136*, 9552–9555. (b) Nardele, C. G.; Dhavale, V. M.; Sreekumar, K.; Asha, S. K. *J. Polym. Sci., Polym. Chem.* **2015**, *53*, 629–641.
- (19) Pecinovsky, C. S.; Hatakeyama, E. S.; Gin, D. L. *Adv. Mater.* **2008**, *20*, 174–178.
- (20) Harris, K. D.; Cuypers, R.; Scheibe, P.; Mol, G. N.; Lub, J.; Bastiaansen, C. W. M.; Broer, D. J. *Proc. SPIE—Int. Soc. Opt. Eng.* **2005**, *5836*, 41–55.
- (21) (a) Bras, W.; Dolbnya, I. P.; Detollenaire, D.; van Tol, R.; Malfois, M.; Greaves, G. N.; Ryan, A. J.; Heeley, E. *J. Appl. Crystallogr.* **2003**, *36*, 791–794. (b) Portale, G.; Cavallo, D.; Alfonso, G. C.; Hermida-Merino, D.; van Drongelen, M.; Balzano, L.; Peters, G. W. M.; Goossens, J. G. P.; Bras, W. *J. Appl. Crystallogr.* **2013**, *46*, 1681–1689.
- (22) Gonzalez, C. L.; Bastiaansen, C. W. M.; Lub, J.; Loos, J.; Lu, K.; Wondergem, H. J.; Broer, D. J. *Adv. Mater.* **2008**, *20*, 1246–1252.
- (23) Herzer, N.; Guneysu, H.; Davies, D. J. D.; Yildirim, D.; Vaccaro, A. R.; Broer, D. J.; Bastiaansen, C. W. M.; Schenning, A. P. H. *J. Am. Chem. Soc.* **2012**, *134*, 7608–7611.
- (24) Shishmanova, I. K.; Bastiaansen, C. W. M.; Schenning, A. P. H. J.; Broer, D. J. *Chem. Commun.* **2012**, *48*, 4555–4557.
- (25) Lagerwall, J. P. F. In *Structures and Properties of the Chiral Smectic C Liquid Crystal Phases*, Göteborg, Sweden, 2002.
- (26) Ruslim, C.; Ichimura, K. *Macromolecules* **1999**, *32*, 4254–4263.
- (27) Yu, W. C.; Sung, C. S. P.; Robertson, R. E. *Macromolecules* **1988**, *21*, 355–364.
- (28) Liu, D.; Bastiaansen, C. W. M.; den Toonder, J. M. J.; Broer, D. J. *Angew. Chem., Int. Ed.* **2012**, *51*, 892–896.
- (29) (a) Priimagi, A.; Shimamura, A.; Kondo, M.; Hiraoka, T.; Kubo, S.; Mamiya, J.-I.; Kinoshita, M.; Ikeda, T.; Shishido, A. *ACS Macro Lett.* **2011**, *1*, 96–99. (b) Cheng, L.; Torres, Y.; Lee, K. M.; McClung, A. J.; Baur, J.; White, T. J.; Oates, W. S. *J. Appl. Phys.* **2012**, *112*, 013513.
- (30) (a) Somer, G.; Green, M. E. *Photochem. Photobiol.* **1973**, *17*, 179–190. (b) Usui, Y.; Koizumi, M. *Bull. Chem. Soc. Jpn.* **1961**, *34*, 1651–1658.